

NEW ATTENUATION RELATIONS FOR PEAK GROUND ACCELERATION AND VELOCITY CONSIDERING EFFECTS OF FAULT TYPE AND SITE CONDITION

Hongjun SI¹ And Saburoh MIDORIKAWA²

SUMMARY

New attenuation relationships for peak ground acceleration on soil ground and for peak ground velocity on stiff ground are developed based on the regression analysis of strong ground motion recordings from 21 Japan earthquakes. In the analysis, 856 data for peak ground acceleration and 394 data for peak ground velocity are used, including those recorded in the near-source area. In the study, the earthquakes are classified into three groups, i.e., crustal, inter-plate and intra-plate earthquakes, according to the fault type. The site effects are evaluated quantitatively, and the path effects are evaluated by using two types of distance measurement, such as fault distance and equivalent hypocentral distance. The new attenuation relationships show that an intra-plate earthquake generates stronger acceleration and velocity than inter-plate and crustal events. The results also show that the earthquake with deeper focal depth generates stronger ground motion.

INTRODUCTION

The prediction of ground motion from a large scenario earthquake is of fundamental importance to earthquake engineering. As an empirical method for the prediction, attenuation relations are frequently employed. Although many attenuation relations have been proposed based on the regression analysis of strong motion recordings, there remain several problems. First, as most of Japan earthquakes are located in the ocean area, the near-source recordings are rarely obtained. Few strong motion data in the near-source area are included in the analysis. Second, it is difficult to express the characteristics of the individual earthquakes in the relation because the factors used in the relation are limited for simplifying the attenuation model, e.g., magnitude for expressing source effects. Recently, it is suggested that the fault type and the focal depth should be taken into account for the source characteristics (McGarr, 1984; Youngs et al., 1997). Third, for the path effects, the appropriate definition of the distance in the near-source area is in controversy (Campbell, 1985). Fourth, for the site effects, it is also suggested that the qualitative evaluation using soil types is not sufficient (Fukushima and Tanaka, 1990; Midorikawa et al., 1994).

In this study, we propose new attenuation relations based on the regression analysis, in which the effects of source, path and site condition on ground motion are considered more precisely. For the purpose, a strong motion database is compiled from the recent Japan earthquakes. The database is featured by the following characteristics: a) a number of near-source recordings is included; b) the magnitude of the earthquakes is widely distributed in a range of 5.8 to 8.3; c) the earthquakes have various fault types; d) the focal depths range from 6 km to 120 km. In the regression model, in addition to the closest distance to the fault plane, the equivalent hypocentral distance (Ohno et al., 1993), a recently proposed distance measurement is also adopted. For evaluating the source effects correctly, we added the fault type and the focal depth as additional factors in the regression model. In the analysis, the site effects are quantitatively evaluated. Finally, attenuation relations for peak ground acceleration (PGA) on soil ground, peak ground velocity (PGV) on stiff ground are developed in this study.

¹ Kozo Keikaku Engineering Inc., Tokyo, Japan Email: shj@kke.co.jp

² Department of Built Environment, Tokyo Institute of Technology, Tokyo, Japan Email: smidorik@enveng.titech.ac.jp

DATABASE

The data from 21 Japan earthquakes occurred in 1968 to 1997 are compiled in the database as shown in Table 1. Figure 1 shows the distribution in moment magnitude and the focal depth. Here, we define the focal depth as an average depth of the fault plane. The focal depths in our database are almost less than 40 km, except one is just over 70 km, and two are deeper than 100 km. Figure 2 shows the histogram of the fault type. The fault type is classified into 3 categories, that are, crustal, inter-plate and intra-plate earthquakes.

In this study, we use the closest distance to the fault plane (refer to as fault distance) and the equivalent hypocentral distance (refer to as EHD) to describe the source-to-site distance. The former is simply defined, and has been often employed in the previous studies. The latter has physical basis, inducing the point source model to be applicable in the near-source area (Ohno et al., 1993). However, as the distribution of displacement over the fault plane is needed for computing the EHD, it is not easy to be routinely obtained.

In the database, there are 1137 PGA data and 543 PGV data. All the data are recorded at free field sites or small buildings where soil-structure interaction effects are negligible. As the data are observed with different types of the instrument, the data are instrumentally corrected with the filter illustrated in Fig.3. In the figure, the corner frequency is given as follows according to the noise level of the data: (a) $F1=0.15 \text{ Hz} \square F2=0.08 \text{ Hz}$; (b) $F1=0.20 \text{ Hz} \square F2=0.10 \text{ Hz}$; or (c) $F1=0.33 \text{ Hz} \square F2=0.15 \text{ Hz}$. The data obviously affected by soil liquefaction, such as the recording at Port Island during 1995 Hyogo-ken Nanbu, Japan earthquake, are removed from the database.

In the analysis, the strong motion data satisfied the following criteria are adopted: distances less than a) 300 km when magnitude greater than 7, b) 200 km when magnitude between 6.6 and 7, c) 150km when magnitude between 6.3 and 6.5, and d) 100 km when magnitude under 6.3. Finally, the data used in the analysis are 856 records for PGA, and 394 records for PGV. The peak ground motion is defined as the larger one of the two horizontal components. In Fig.4, distributions in moment magnitude and fault distance of the data set for PGA and PGV are illustrated. In the figure, it can be confirmed that a number of near-source recordings is included.

To evaluate the site effects on ground motion, we compiled the soil profiles at the observation stations. First, we classified soil characteristics into two categories, rock and soil, for all the observation stations. The definition of rock and soil is after Joyner and Boore (1981). For the stations with more details of soil profile, we calculate the average shear wave velocity from surface to a depth of 30m [refer to as AVS30 hereafter] at the site. The AVS30 is computed by dividing the depth by the summation of the travel times of soil layers.

REGRESSION ANALYSIS

Regression Model

Two regression models are used in the analysis. One is for fault distance shown in Eq. (1), another one is for EHD shown in Eq. (2).

$$\log A = b - \log (X + c) - k X \quad (1)$$

$$\log A = b - \log X_{eq} - k X_{eq} \quad (2)$$

where, A is peak ground motion, X is fault distance in km, and X_{eq} is EHD in km. The first term in Eqs. (1) (2), i.e., the coefficient b is an offset factor for each earthquake. The second term shows geometrical attenuation, and the third term shows anelastic attenuation. For the coefficient k , we fix at 0.003 for PGA and 0.002 for PGV. For the case of fault distance, coefficient c is introduced accounting for the saturation of the amplitude of strong motion in the near-source area. The coefficient c is given as a function of magnitude;

$$c = c_1 10^{c_2 M_w} \quad (3)$$

Evaluation of Site Effects on Strong Motion

Recent studies (Campbell, 1991; Midorikawa et al., 1994) indicated that the average amplitude of PGA at soil sites is about 1.4 times greater than that at rock sites. In the light of these results, we convert the PGA at a rock site to that at a soil site by multiplying the value with a factor of 1.4. We develop the attenuation relation for PGA on soil ground because most of the data used in this study are observed at soil sites.

For PGV, Midorikawa et al. (1994) proposed a method for the evaluation of site effects. As shown in Eq. (4), the site amplification factor R is calculated with AVS30. The PGV at stiff site [V_{cor}] is calculated by dividing the observed PGV [V_{org}] by R as shown in Eq. (5). The stiff site means that the site amplification factor R shown in Eq. (4) is 1, i.e., the AVS30 is about 600 m/s. We propose the attenuation relation for PGV on stiff ground.

$$\log R = 1.83 - 0.66 \log AVS30 \quad (4)$$

$$V_{cor} = V_{org} / R \quad (5)$$

Method

In developing the attenuation relations, we adopted a two-stage regression method. In the first stage, regression models shown in Eqs. (1) and (3) or Eq. (2) are fitted to the data from each earthquake, gaining the value of coefficient b . For stronger reflection of the near-source records, we weighted the data closer than 25 km by a factor of 8, 20 – 50 km by 4, 50 – 100 km by 2, and farther than 100 km by 1. For the case of fault distance, the value of c is difficult to be determined for all the events because of limited number of the near-source recordings. Here, at first we determined the value of c for the earthquakes with sufficient near-source data, then develop a regression equation of c as a function of magnitude. Substituting the function to the regression model, the coefficient b can be obtained. In the second stage, selecting magnitude, the fault type and the focal depth as the parameters, the regression equation of b is precisely derived.

RESULTS

Analysis without Constraints

Coefficient c in Eq. (1) for PGA and PGV is obtained in the regression analysis of the near-source data from 3 and 4 earthquakes, respectively. The value of coefficient c for each earthquake is plotted versus moment magnitude in Figs. 5 and 6. In the diagrams, the data of coefficient c obtained from the sufficient near-source data are plotted with circles. The data of coefficient c from less near-source data, and the datum derived from the 1985, Chile earthquake (Midorikawa, 1991) are plotted with triangles. In the regression analysis of the data with model shown in Eq. (3), we derived the relation of the coefficient c and magnitude, as shown in Eq. (6) and (7), for PGA and PGV, respectively.

$$c = 0.0055 \cdot 10^{0.50M_w} \quad (\text{for PGA}) \quad (6)$$

$$c = 0.0028 \cdot 10^{0.50M_w} \quad (\text{for PGV}) \quad (7)$$

In Figs. 5 and 6, the results by Fukushima and Tanaka (1992), and by Nozu et al. (1997) are also plotted. The results are consistent with those in this study.

By fitting the data from each earthquake to the equation (1) and (6) or (7), the value of coefficient b is obtained. As an example of the fitting, Figures 7 show the data of PGA and PGV from the 1995 Hyogo-ken Nanbu, Japan earthquake, and the fitting curve with the regression model. Figures 8 show the relation between coefficient b and moment magnitude. From the figure, there is strong correlation between coefficient b and magnitude. In the figure, however, with the same magnitude, the coefficient b has different values. This implied that, in addition to the magnitude, there are still other factors that affect strong ground motion. Referring to the previous studies, the focal depth and the fault type are considered as the additional factors. In order to obtain a precise equation about the coefficient b , a model shown as Eq. (8) is employed.

$$b = aM_w + hD + \sum d_i S_i + e + \varepsilon \quad (8)$$

where, D is focal depth in km, S_i is fault type, ε is the standard deviation. a , h , d and e is the regression coefficient. S_i is a dummy variable, with the value of 1 for each fault type as described in the previous part and 0 for the others. We weighted the data in the analysis according to the number of recordings for each earthquake. The weighting factor is set as 3 for the earthquake with mark A in Table 1, 2 for B and 1 for C.

The coefficients in Eq. (8) derived from the regression analysis are shown in Table 2. For the case of EHD, the results are listed in Table 3.

Analysis with Constraints

In our database, it is remarkable that there is correlation among the parameters in the regression model. For example, the earthquake with larger magnitude has deeper focal depth. Because of this, coefficients a and h may not be correctly determined. Comparing with the results shown in Table 3 for EHD, the results shown in Table 2 for fault distance show larger value of coefficient a for M_w and smaller value of the coefficient h for focal depth. This is considered to be the influence of the trade-off.

At sites far from the earthquake source, the predicted strong motions by the attenuation relations should be the same in spite of the difference of distance measurement. For this reason, in the attenuation relations with different distance measurement, the values of coefficient a for magnitude are likely to be the same. Here, we assign this to a constraint for the regression analysis. In recent studies, it is indicated that the PGA at the near-source sites should be almost the same in spite of the difference of magnitude. Thus, We adopted an additional constraint in the analysis, that is, the predicted PGAs are the same at the sites where the distance is zero.

With these constraints, by performing the regression analysis again, we derived the new results, as shown in Tables 4 and 5. Substituting the coefficients into the attenuation models, we obtained the new attenuation relations for PGA and PGV. The log-scaled standard deviations of the new attenuation relations are shown in Table 6. The standard deviations in this study are less than 0.25 for the distances less than 100 km. It suggests that the new attenuation relations fitted the data very well.

Predicted Strong Ground Motions

In Figs.9, the attenuation curves are illustrated for the inter-plate earthquakes, with focal depth of 5 km, magnitudes of 6.0 to 8.0, respectively. In the figures, the attenuation curves for PGA show small magnitude dependencies, but those for PGV show stronger one. This is consistent with the results in the previous studies. In Figs.10, the attenuation curves are illustrated for the intra-plate earthquakes with magnitude of 7. The focal depths are set to 30 km and 100 km. In the figure, the predicted PGA and PGV for the focal depth of 100 km is about 2 and 1.8 times greater than those for the focal depth of 30 km, respectively. In Figs.11, the attenuation curves are illustrated for the earthquakes with different fault types. The magnitude is 7, and the focal depth is 20 km. In the figure, the predicted PGA and PGV for the intra-plate event is about 1.7 and 1.4 times greater than those for the crustal and inter-plate events, respectively.

In Figs.12 and 13, we compare the attenuation relations proposed in this study and those in the previous studies (Boore et al., 1997; Campbell, 1997; Youngs et al., 1997; Fukushima and Tanaka, 1992; Annaka et al., 1997; Ohta and Ohno, 1996; Joyner and Boore, 1982; and Kawashima et al., 1985). The comparisons are carried out for the case of fault distance and EHD, respectively. The predicted curves by the relations in this study are calculated for the earthquake that M_w is 7, the focal depth is 5 km, and the fault type is crustal earthquake. In the figure, the results in this study are consistent with those proposed by the previous studies.

CONCLUSIONS

New attenuation relationships for peak ground acceleration on soil ground and for peak ground velocity on stiff ground are developed based on the regression analysis of strong ground motion recordings from 21 Japan earthquakes. In the analysis, 856 data for peak ground acceleration and 394 data for peak ground velocity are used, including those recorded in the near-source area. In the study, the earthquakes are classified into three groups, i.e., crustal, inter-plate and intra-plate earthquakes, according to the fault type. The site effects are evaluated quantitatively, and the path effects are evaluated by using two types of distance measurement, such as fault distance and equivalent hypocentral distance. The new attenuation relationships show that an intra-plate earthquake generates stronger acceleration and velocity than inter-plate and crustal events. The results also show that the earthquake with deeper focal depth generates stronger ground motion.

ACKNOWLEDGEMENTS

The authors thank the following organizations for providing the strong motion data and site information: Building Research Institute, Central Research Institute of Electric Power Industry, Electric Power Development Co., Fire Research Institute, Fujita Co., Hachinohe Institute of Technology, Hazama Co., Hokkaido Electric Power Co., Hirosaki University, Hokkaido University, Japan Meteorological Agency, Kajima Co., Kanagawa Prefecture Government, Kanagawa University, Kansai Electric Power Co., K-NET, Kumagai Co., Kyoto University, Mitsubishi Estate Co., Matsumura-Gumi, Mitui Co., National Research Institute For Earth Science

and Disaster Prevention, Nishimatsu Constr., NTT, Obayashi Co., Osaka Gas Co., Port and Harbour Research Institute, Public Work Research Institute, Railway Technical Research Institute, Sato Kogyo Co., Shimizu Co., Takenaka Co., Committee of Earthquake Observation and Research in the Kansai Area, Tobishima Co., Tokyo Gas Co., Tokyo Metropolitan Government, Tokyo Electric Power Co., Tokyo Institute of Technology, Tokyo Constr., University of Tokyo, and Waseda University.

REFERENCES

- Annaka, M., F. Yamazaki, and F. Katahira (1997), "A proposal of estimation equations for peak ground motion and response spectral using the data recorded by JMA87 seismograph", *Proceedings of the 24th JSCE Earthquake Engineering Symposium*, pp. 161-164 (In Japanese)□
- Boore, D.M, W.B. Joyner, and T.E. Fumal (1997), "Equations for estimating horizontal response spectra and peak acceleration from Western North American earthquakes: a summary of recent work", *Seism. Res. Lett.*, Vol.68, pp.128-153.
- Campbell, K.W (1985), "Strong motion attenuation relations: a ten-year perspective", *Earthquake Spectra*, Vol.1, pp.759-804□1985□
- Campbell, K.W. (1991), "An empirical analysis of peak horizontal acceleration for the Loma Prieta, California, earthquake of 18 October 1989", *Bull. Seism. Soc. Am.*, Vol.81, pp.1938-1858.
- Campbell, K.W. (1997), "Empirical near-source attenuation relationships for horizontal and vertical components of peak ground acceleration, peak ground velocity, and pseudo-absolute acceleration response spectra", *Seism. Res. Lett.*, Vol. 68, pp.154-179.
- Fukushima, Y. and T. Tanaka (1990), "A new attenuation relation for peak horizontal acceleration of strong earthquake ground motion in Japan", *Bull. Seism. Soc. Am.*, Vol.80, pp.757-783.
- Fukushima, Y. and T. Tanaka (1992), "Revised attenuation relation of peak horizontal acceleration by using a new data base", *Program and Abstracts of the Seism. Soc. Japan*, No.2, p.116. (In Japanese)
- Kawashima, K., K. Aizawa and K. Takahashi (1985), "Attenuation relations for peak ground motion and response spectral", *Tech. Memorandum of Public works Res. Inst.*, No.166 (In Japanese).
- Joyner, W.B. and D.M. Boore (1981), "Peak horizontal acceleration and velocity from strong motion records including records from the 1979 Imperial Valley, California, earthquake", *Bull. Seism. Soc. Am.*, Vol.71, pp.2011-2038.
- Joyner, W. B. and D. M. Boore (1982), "Prediction of earthquake response spectra", *U.S. Geol. Surv. Open-File Rept.*, No.82-977.
- McGarr, A. (1984), "Scaling of ground motion parameters, state of stress, and focal depth", *J. Geophys. Res.*, Vol.89, pp.6969-6979.
- Midorikawa, S. (1991), "Attenuation of the peak ground acceleration and velocity during the 1985 Chile and Nihonkai-chubu earthquakes", *Journal of Struct. Construct. Eng.*, No.422, pp.37-44 (in Japanese, with English abstract).
- Midorikawa, S., M. Matsuoka and K. Sakugawa (1994), "Site effects on strong-motion records during the 1987 Chiba-ken-toho-oki□Japan earthquake", *The 9th Japan Earthquake Engineering Symposium*, Vol.3, pp. 85-90.
- Molas, G.L. and F. Yamazaki (1995), "Attenuation of earthquake ground motion in Japan including deep focus events", *Bull. Seism. Soc. Am.*, Vol.85, pp.295-319.
- Nozu, A., T. Uwabe, Y. Sato, K. Ichii, and S. Iai (1997), "Attenuation relations for peak ground motions on base layer in Japan", *Proceedings of Earthquake Criteria Workshop -Recent Developments in Seismic Hazard and Risk Assessments for Port, Harbor, and Offshore Structures-*, pp.118-135.
- Ohno, S., T. Ohta, T. Ikeura, and M. Takemura (1993), "Revision of attenuation formula considering the effect of fault size to evaluate strong motion spectra in near field", *Tectonophysics*, Vol.218, pp.69-81.
- Ohta, T. and S. Ohno (1996), "Average characteristics of earthquake ground motions in and around focal region based on strong motion records", *Journal of Struct. Construct. Eng.*, No.479, pp.31-40 (in Japanese).
- Tanaka, T., and Y. Fukushima (1987), "Attenuation relations for peak amplitudes of earthquake ground motions", *Proc. 15th Earthq. Ground motion Symp.*, Architectural Institute of Japan, pp.7-16 (in Japanese).
- Youngs, R.R., S.J. Chiou, W.J. Silva, and J.R. Humphrey (1997), "Strong ground motion attenuation relationships for subduction zone earthquakes", *Seism. Res. Lett.*, Vol.68, pp.58-73.

Table 1. The list of the data compiled in the database

NO.	Earthquake	Date	M_w	Depth	Number of recordings		Fault Type	Weight
					Peak acceleration	Peak velocity		
1	Off Tokachi	1968.05.16	8.2	15	10	10	Inter-plate	C
2	Off Nemuro Pen.	1973.06.17	7.8	25	6	4	Inter-plate	C
3	Near Izu Oshima	1978.01.14	6.6	7	8	12	Crustal	C
4	Off Miyagi Pref.	1978.06.12	7.6	37	13	10	Inter-plate	C
5	East off Izu Pen.	1980.06.29	6.5	7	19	16	Crustal	B
6	Off Urakawa	1982.03.21	6.9	25	19	9	Crustal	C
7	Nihonkai-Chubu	1983.05.26	7.8	6	21	17	Inter-plate	C
8	Off Hyuganada	1984.08.07	6.9	30	9	8	Intra-plate	C
9	Central Iwate Pref.	1987.01.09	6.6	73	10	5	Intra-plate	C
10	Northern Hidaka Mt.	1987.01.14	6.8	120	16	9	Intra-plate	C
11	East off Chiba Pref.	1987.12.17	6.7	30	173	47	Crustal	A
12	Off Kushiro	1993.01.15	7.6	105	51	21	Intra-plate	B
13	Off Noto Pen.	1993.02.07	6.3	15	21	5	Crustal	C
14	Southwest off Hokkaido	1993.07.12	7.7	10	52	18	Inter-plate	B
15	East off Hokkaido	1994.10.04	8.3	35	41	17	Intra-plate	B
16	Far off Sanriku	1994.12.28	7.7	35	83	30	Inter-plate	B
17	Hyogo-ken Nanbu	1995.01.17	6.9	10	85	47	Crustal	A
18	Off Hyuganada	1996.10.19	6.7	25	106	67	Inter-plate	A
19	Northwestern Kagoshima Pref.	1997.03.26	6.1	6	121	68	Crustal	A
20	Northwestern Kagoshima Pref.	1997.05.13	6.0	7	121	64	Crustal	A
21	Northern Yamaguchi Pref.	1997.06.25	5.8	10	152	59	Crustal	A

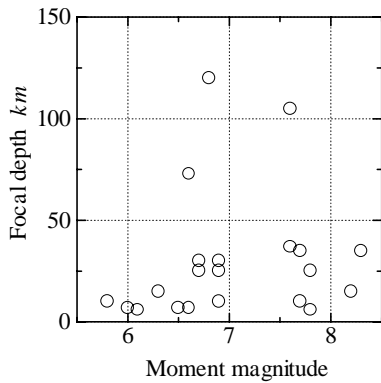


Fig.1. Focal depth vs. M_w

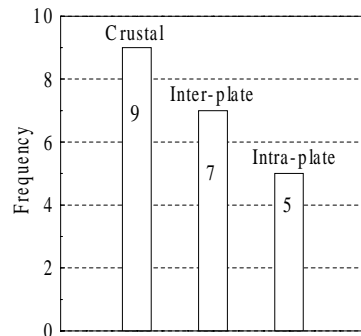


Fig.2. Histogram of the fault types

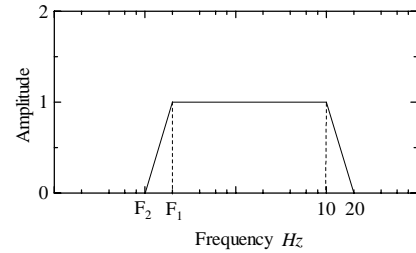


Fig.3. Band-pass filter used for instrument correction

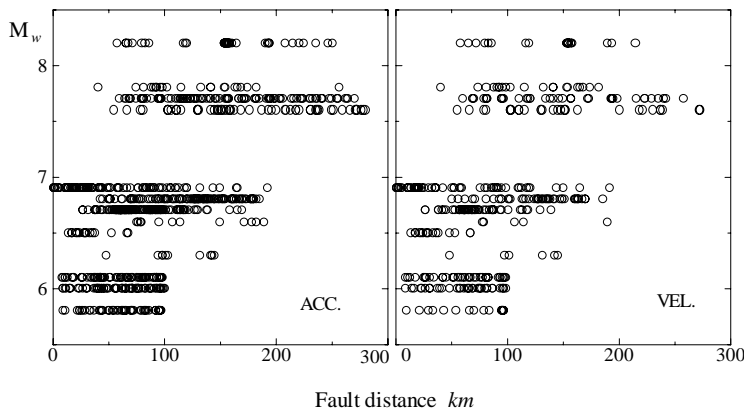


Fig.4. Fault distance vs. M_w

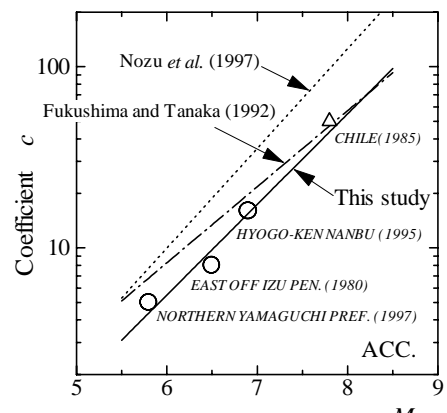


Fig.5. Coefficient c for peak ground acceleration

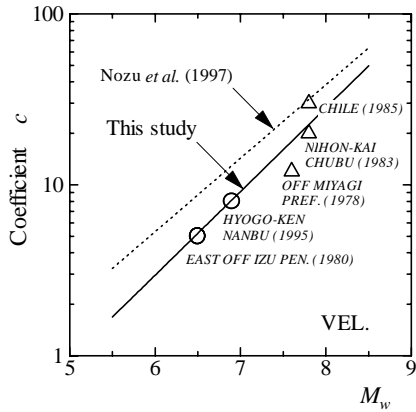


Fig.6. Coefficient c for peak ground velocity

Table 2 The results for fault distance (without constraints)

a	h	d			e
		Crustal	Inter-plate	Intra-plate	
Peak ground acceleration					
0.53	0.0044	0.00	-0.04	0.17	0.38
Peak ground velocity					
0.55	0.0037	0.00	0.01	0.16	-1.10

Table 3 The results for EHD (without constraints)

a	h	d			e
		Crustal	Inter-plate	Intra-plate	
Peak ground acceleration					
0.58	0.0039	0.00	0.01	0.18	0.12
Peak ground velocity					
0.60	0.0032	0.00	0.03	0.13	-1.39

Table 4 The results for fault distance (with constraints)

a	h	d			e
		Crustal	Inter-plate	Intra-plate	
Peak ground acceleration					
0.50	0.0036	0.00	0.09	0.28	0.60
Peak ground velocity					
0.58	0.0031	0.00	0.06	0.16	-1.25

Table 5 The results for EHD (with constraints)

a	h	d			e
		Crustal	Inter-plate	Intra-plate	
Peak ground acceleration					
0.50	0.0043	0.00	0.01	0.22	0.61
Peak ground velocity					
0.58	0.0038	0.00	-0.02	0.12	-1.29

Table 6. The standard error for the proposed attenuation relations

Standard error	Equivalent hypocentral distance		Fault distance	
	P.G.A.	P.G.V.	P.G.A.	P.G.V.
All data	0.28	0.23	0.27	0.23
D ... 100km	0.24	0.22	0.25	0.23

D = distance

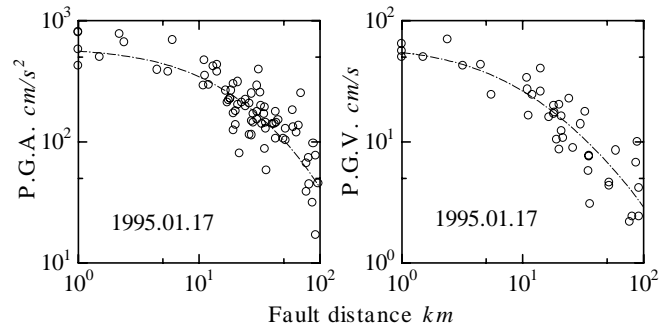


Fig.7. Examples of fitting the data with the regression model

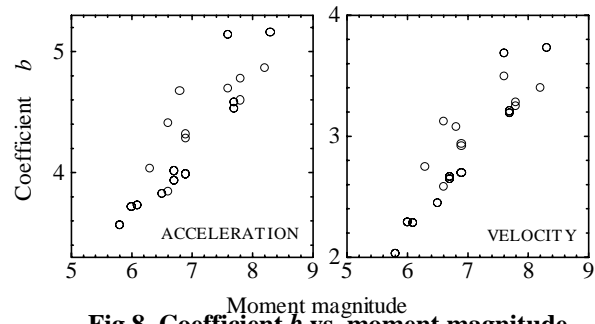


Fig.8. Coefficient b vs. moment magnitude

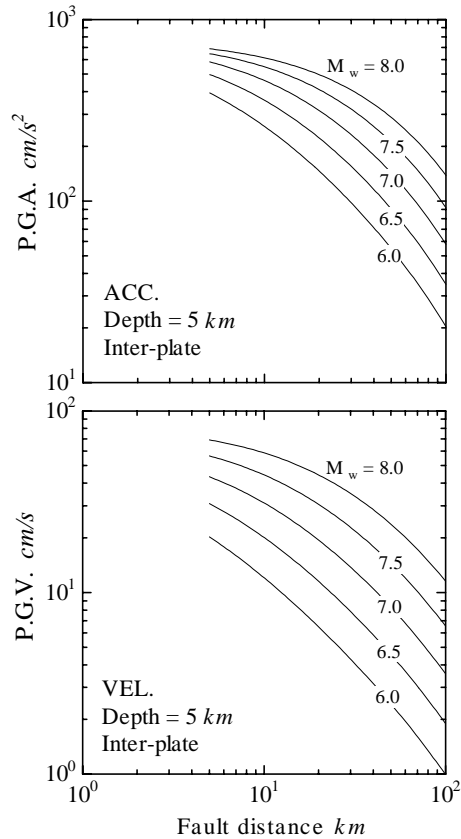


Fig.9. Predicted attenuation curves

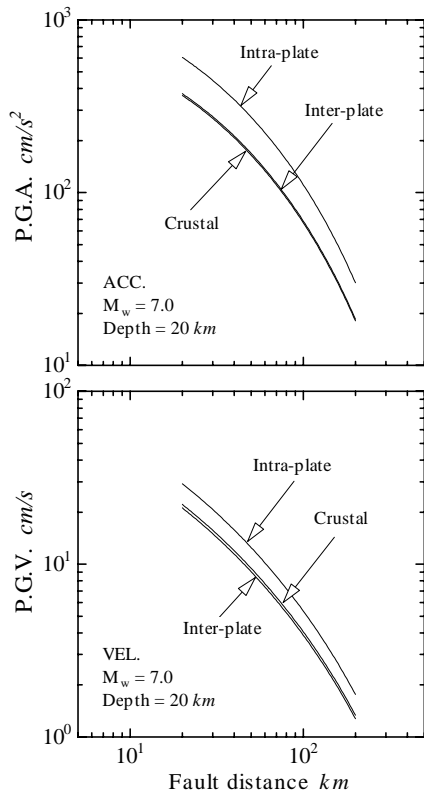


Fig.10. The effects of focal depth on strong motion

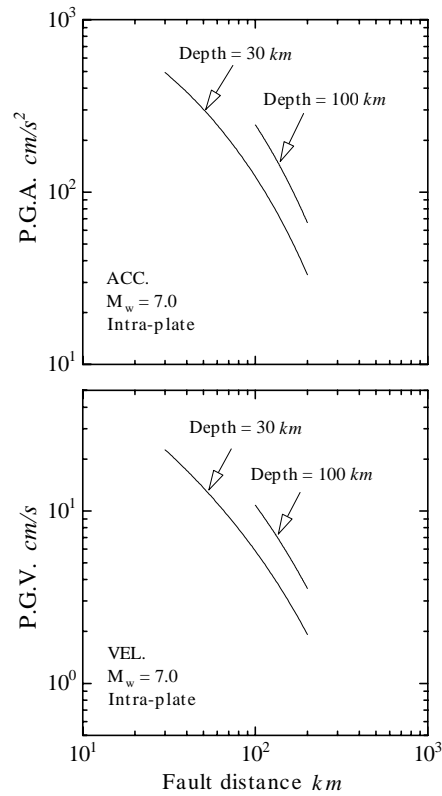


Fig.11. The effects of fault type on strong motion

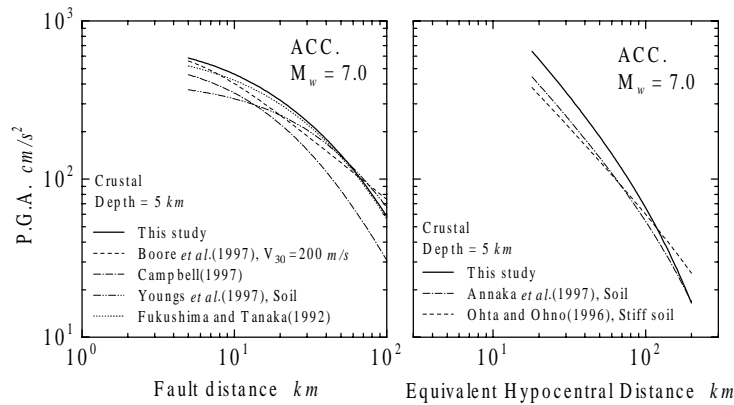


Fig.12. Comparison of the attenuation relations for peak ground acceleration

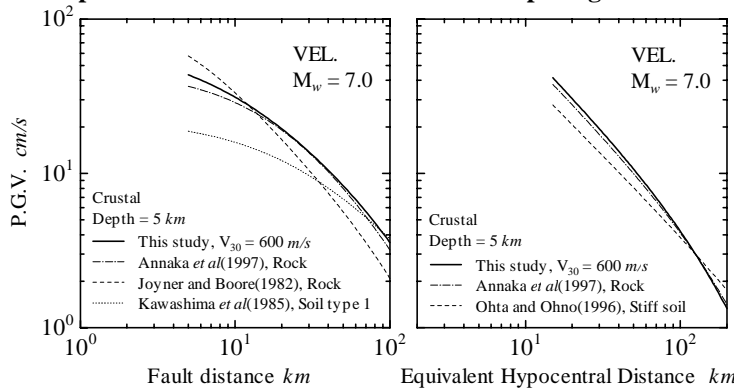


Fig.13. Comparison of the attenuation relations for peak ground velocity